IGHEM 2016

Flow Comparison Test at GM Shrum Powerplant

John W. Taylor, Allium Hydrotech, Vancouver, BC, Canada;

David D. Lemon and Dave Billenness, ASL AQFlow, Victoria, BC, Canada

Abstract

This paper describes the results of a recent large scale flow comparison test undertaken at BC Hydro's GM Shrum powerplant. The test compared two methodologies: acoustic time of travel (ATT) and acoustic scintillation (AS). Both of these methodologies are in use in the hydropower world particularly for contract turbine efficiency tests. The AS method is more economical when testing more than one unit at a plant because the measurement frame can easily be moved from intake to intake.

GM Shrum powerplant consists of 10 Francis units providing a total of about 2700 MW. It has an underground powerhouse and a head of 161 m. The penstock diameter is 5 m.

BC Hydro has recently upgraded five units, all under a single contract. An efficiency test was undertaken on only one of the five units using the ATT flowmeter as specified in the turbine contract. However BC Hydro wanted to test the remaining 4 uprated units so that measured efficiencies could be used to optimize the dispatch from the plant. There may be small efficiency differences between the units due to different intake layouts and small turbine fabrication differences. If the ATT flowmeter were used for these tests, transducers would have to be installed in all four penstocks.

Instead, for economic reasons, BC Hydro opted to consider testing the 4 units using an AS flowmeter. The comparison test described in this paper was meant to verify that the two flowmeters are comparable at this powerplant, by carrying out the flow comparison measurements at the unit for which the efficiency test was performed.

The paper describes the differences found between the two flowmeters and the stability of outputs over a range of flows. It also describes the challenges in undertaking a large scale comparison test like this.

Introduction

GM Shrum generating station is located on the Peace River in northeastern British Columbia and supplies 12% of the energy BC Hydro generates in the province.

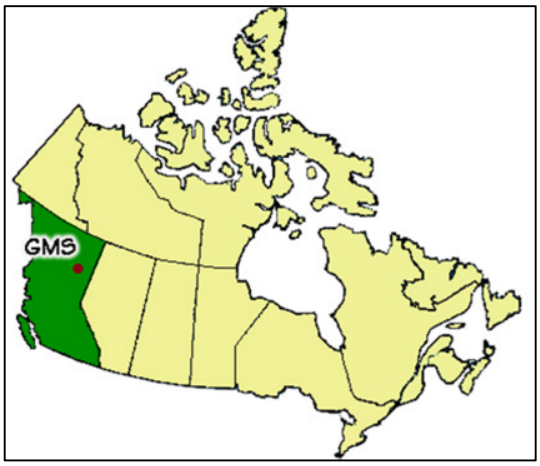

Figure 1: Location map and view of WAC Bennet Dam and GM Shrum Generating Station

The dam and powerplant were built in the early 1970s. The underground powerhouse has 10 Francis units providing a total of about 2730 MW. The net head is 161 m and the penstock diameter is 5 m. Recently, BC Hydro upgraded 5 units with new turbines. One of the new units was efficiency tested to meet contract requirements, using an Acoustic Travel Time (ATT) flow meter in the penstock. The remaining 4 units were not tested, as their penstocks were not equipped with flow meters, and the cost of installing them was considered prohibitive. Of the remaining 6 older units in the plant, only 3 have been tested.

BC Hydro would like to test the remaining units so that measured efficiencies could be used to manage dispatch from the plant. Even among the upgraded units, there may be small efficiency differences between the units. The potential differences are even larger among the remaining 6 older units, so it is considered desirable to test all units on the same basis. A 0.2% improvement in plant dispatch at GM Shrum is worth approximately $1.1 million per year.

Flow measurement is a critical part of efficiency testing, but can also be costly to perform at plants like GM Shrum if instrumentation has to be installed in each penstock. A recent BC Hydro study (Taylor et al, 2012) compared the cost of turbine efficiency testing at multiunit plants with ATT, current-meter and AS methods. Because fully instrumented AS frames can be moved from unit to unit at little extra cost (no unit dewatering, no equipment dismantling and reinstallation), the unit testing cost with AS was indicated to be less than 50% of the testing cost with ATT if the 4 units were tested consecutively. A consecutive testing of all 10 units would result in even more cost reduction. If only the flow measurement costs are considered, the

incremental cost of testing additional units with the AS method would be only about 20% of the same testing with the ATT method (Taylor et al, 2012). BC Hydro therefore is considering using acoustic scintillation (AS) for measuring flow at the rest of the GM Shrum units. That flexibility and ease of installation is also an advantage for longer-term monitoring, as repeat flow measurements are easily done.

Before deciding whether or not to proceed with a multi-unit testing program using the AS method, BC Hydro carried out a flow comparison test at the upgraded turbine (Unit 4) that had been tested for contract acceptance, as it had an ATT system in place. Experience with other comparison tests had shown that the two methods usually agreed with each other to within 1%, however verification that the AS system could perform accurately at the GM Shrum plant was desired, as the flow speeds in the intake and penstock were significantly higher than previously encountered with the AS method. Figure 2 shows the locations of the two instruments at Unit 4.

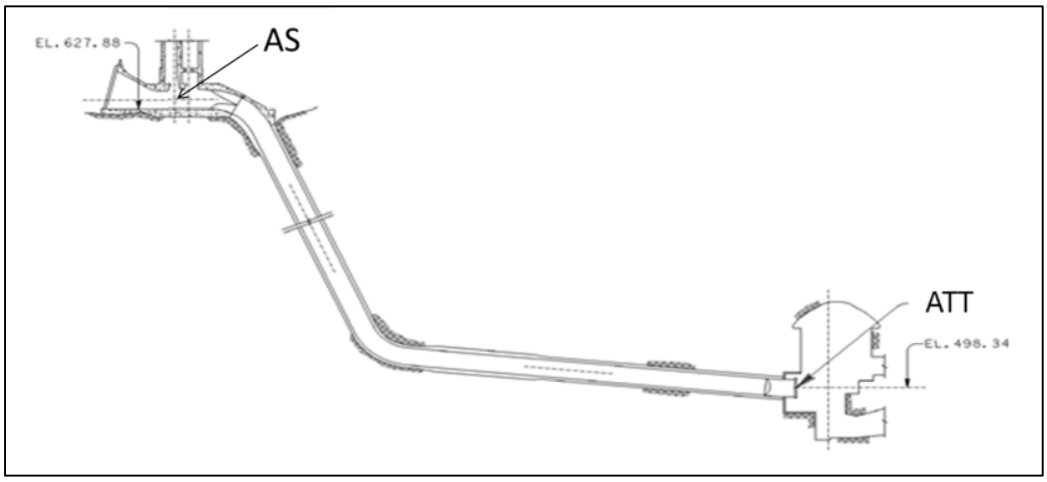

Figure 2: Location of the two methods at Unit 4

Acoustic Scintillation Method

Principle of Operation

The AS method uses a technique called acoustic scintillation drift (Clifford & Farmer, 1983; Farmer & Clifford, 1986; ASL, 2001) to measure the flow velocity perpendicular to a number of acoustic paths established across the intake to the turbine. Short pulses (16 μsec) of high-frequency sound (307 kHz) are sent from transmitting arrays on one side to receiving arrays on the other, at a rate of approximately 300 pings per second. Fluctuations in the amplitude of those acoustic pulses result from turbulence in the water carried along by the current. The instrument measures those fluctuations (known as scintillations) and from them computes the lateral average of the velocity along the conduit axis.

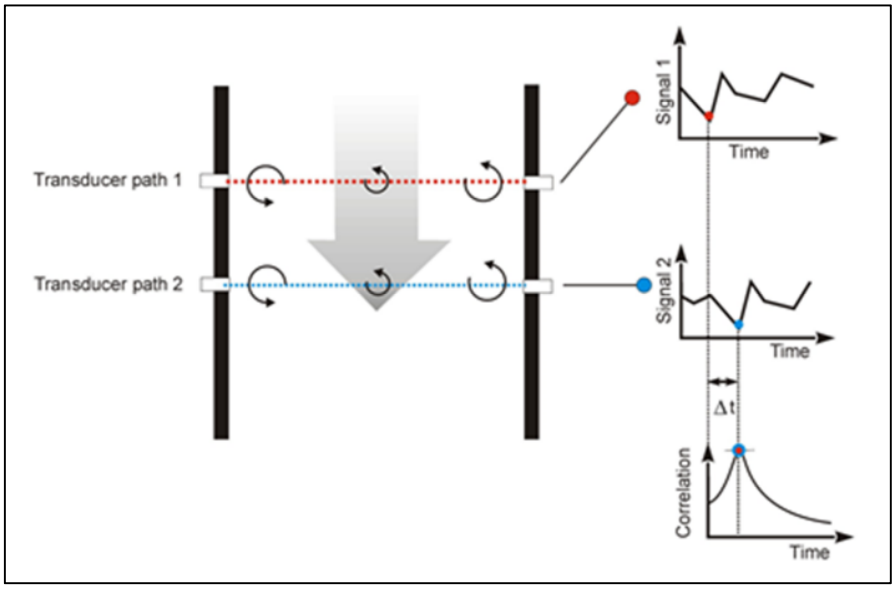

Figure 3: Schematic representation of acoustic scintillation drift.

AS utilizes the natural turbulence embedded in the flow, as shown in Figure 3. In its simplest form, two transmitters are placed on one side of the measurement section, two receivers at the other. The signal amplitude at the receivers varies randomly as the turbulence along the propagation paths changes with time and the flow. If the two paths are sufficiently close (Δx), the turbulence remains embedded in the flow, and the pattern of these amplitude variations at the downstream receiver will be nearly identical to that at the upstream receiver, except for a time delay, Δt. This time delay corresponds to the peak in the time-lagged cross-correlation function calculated for Signal 1 and Signal 2. The mean velocity perpendicular to the acoustic paths is then $\Delta x/\Delta t$. Using three transmitters and three receivers at each measurement level allows both the magnitude and inclination of the velocity to be measured. The instrument computes the discharge through the intake by integrating the horizontal component of the velocity over the cross-sectional area of the intake.

Implementation at GM Shrum

The ASFM was installed with 16 fixed acoustic paths mounted on a frame in the maintenance gate slot at Unit 4. Plan and vertical section views of the Unit 4 intake are shown in Figure 4.

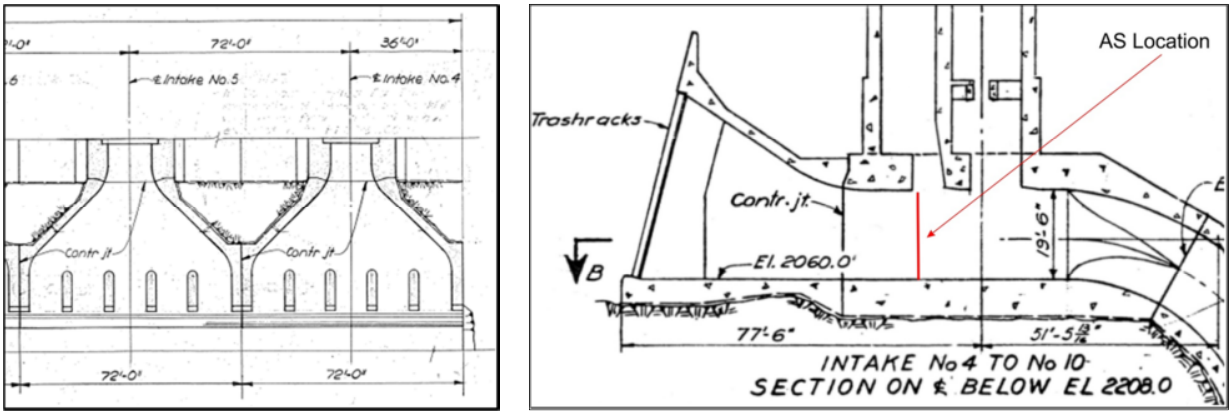

Figure 4: Plan (left) and vertical (right) section views of the Unit 4 intake.

The rows of holes on the frame for the ASFM transducers were placed at the upstream edge of the side faces; the centerline of the arrays was ~13 cm downstream of that edge. The transducers were placed with their faces flush with the sides of the frame so that the full width of the intake was sampled and that they were protected from any debris carried along with the flow.

The maximum flow speeds at GMS (>7.5 m/s) were beyond the upper limit for the standard configuration of the acoustic scintillation instrument, and therefore the test required some modifications to the data collection and processing to maintain accuracy in measuring the flow speed and direction. At the maximum speeds, the cross-correlation peak becomes narrower (in the time domain) and there are fewer measured points to use when interpolating to determine the peak position. The ping rate of the instrument was raised to 300 Hz from 250 Hz, and a revised peak fitting routine for sparse data sets was developed.

Acoustic Time of Travel (ATT)

The ATT system consisted of a Rittmeyer Risonic 2000 flowmeter. The flowmeter transducers were mounted in the penstock just upstream of the spiral case at a location half a pipe diameter downstream of a gradual vertical bend (5°43'). The diameter there is 4.897m. The transducers were installed in 2 planes with 4 horizontal paths each. The paths are oriented at nominally 65° to the penstock axis. Two planes are required to eliminate errors due to non-axial flow in the penstock. Scaling for the flowmeter is based on as-built measurements of path angle, path length, and length of protrusion of the transducers into the flow. The time of travel of a 1 MHz acoustic pulse between two transducer faces is measured in the upstream and downstream directions. The difference in the times of travel is a measure of the axial velocity superimposed on that path. After determining the axial velocity at all four paths in a plane the velocities are integrated vertically into flow using the Gauss Legendre formulation. The calculated flow in each plane is then averaged to determine the flow in the penstock.

Test Procedure

The flow comparisons were carried out in conjunction with other engineering tests being performed on the turbine. Repeat measurements were done at three different flows, with nominal power outputs of 185, 230 and 275 MW. Measurements were also made at other flows, when the engineering test program presented opportunities to do so; however repeat measurements for these tests could not usually be accommodated.

The comparisons were conducted as a blind test for the acoustic scintillation method. BC Hydro personnel filled the role of Chief of Test and operated the ATT instrument. The acoustic scintillation flows were reported to the test chief, but the ATT data were not shared with the AS team until after the test results were finalized. During the test, the AS team was to be notified if flow discrepancies were present that might indicate an instrument malfunction.

The duration of the test at each setting was 20 minutes, during which data were collected simultaneously on both flowmeters. The ATT flow used for comparison was the average over that 20 minute period.

Discharge Computation

Acoustic Scintillation

The roof and floor of the intake and the sides of the frame holding the ASFM transducers define a plane surface, S, through which the flow must pass. The discharge is therefore given by the flux through S:

$$Q = \oint_S \boldsymbol{V} \cdot \boldsymbol{n} \quad da \tag{1}$$

where V is the velocity vector (a function of position in the plane) and n is the unit vector normal to the plane. The ASFM measures the lateral average of the component of velocity normal to the propagation path; if z′ is the vertical coordinate, then the discharge, Q, in terms of the laterally-averaged velocity, v, is:

$$Q = \int_0^H v(z')\cos\left[\theta(z')\right] \cdot L \quad dz' \tag{2}$$

where v(z′) is the magnitude of the laterally-averaged velocity at elevation z′, θ(z′) is the corresponding inclination angle, L(z′) is the width between the transducer faces, and H is the height of the intake roof above the floor for the horizontal paths. The lateral averaging

performed by the ASFM is continuous, while the sampling in the vertical was at sixteen discrete points. Calculating Q then requires estimation of the integral in equation 2 when the integrand is known at a finite number of points. The integral was evaluated numerically using an adaptive Romberg integration, with a quadratic interpolation in the integrand between the measured points. The accuracy of the integration depends on the sampling levels being placed properly to resolve the variation of the horizontal velocity with elevation; 16 paths were used in this case to ensure that any such variations were fully resolved. The measured points do not extend all the way to the intake roof and floor; as a result, complete evaluation of the integral requires an evaluation of the flow in the zones next to those boundaries.

In the field, the acoustic scintillation test team was notified that a discrepancy existed between the two discharge methods, but with no other information. The field results were reviewed after completion of the tests. No changes were made to the velocity data, but the values used for the intake geometry and the boundary layer flow estimates were modified. BC Hydro was able to provide better drawings of the intake, which showed that the roof elevation at the downstream edge of the stoplog slot was 10 cm higher than the upstream edge. The measurement plane is located ~13 cm downstream of the upstream edge of the slot and it is unlikely that the velocity will be zero at the elevation of the upstream edge (5.944 m) since there is no physical boundary in the measurement plane in the roof region and the flow will expand into the open gate slot. It was assumed that the expansion of the flow into the slot would initially follow a steeper trajectory than the straight line joining the upstream and downstream roof edges, and therefore the roof elevation Z_r was increased by 2.5 cm (to 5.970 m) to account for this expansion of the flow into the gate slot.

The boundary layer forms had been set to the same shape and thickness as had been used at the 2009 comparisons at Kootenay Canal (Almquist et al, 2011), however during the review it was realized that the very strong horizontal contraction of the intake (5:1) and the resulting high acceleration of the flow (Figure 5) would significantly reduce the boundary layer thickness.

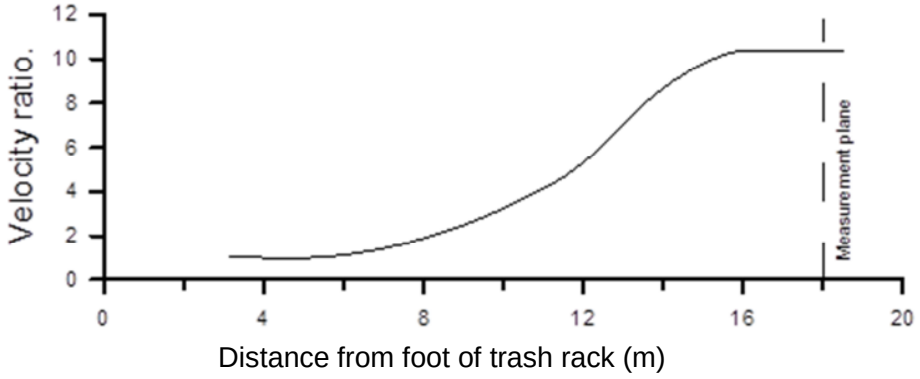

Figure 5: Flow acceleration in the intake at GMS.

Boundary Layer Recalculation

The calculations are based on the method of calculation of general two-dimensional boundary layers presented by Schlichting (1958) and applied to aerofoil boundary layers. The calculations are performed in terms of the integral thicknesses of momentum (θ) and displacement (δ^*), measures which describe the integrated loss of momentum and volume flux within the boundary layer,

$$\delta^* = \int_0^\infty \left(1 - \frac{u}{U}\right) dy \quad \text{and} \quad \theta = \int_0^\infty \frac{u}{U}\left(1 - \frac{u}{U}\right) dy \tag{3}$$

The momentum balance is described by the following equation

$$\frac{d\theta}{dx} + (H+2)\theta \frac{1}{U}\frac{dU}{dx} = \frac{\tau_o}{\rho U^2} \tag{4}$$

where H is the velocity profile shape parameter δ^*/θ, slowly varying such that (H+2) can be regarded as a constant, τ_o is the wall skin friction and ρ is density. The factor $\frac{1}{U}\frac{dU}{dx}$ is known from the intake geometry, and to complete the solution the skin friction term must be expressed in terms of the momentum thickness θ. A power law form was assumed for wall boundary layer profile and the wall stress calculation was adopted from fully rough pipe flow.

Solutions for the roof and floor boundaries are shown in Figure 6 expressed in terms of the displacement thickness δ^* which is a direct measure of the effective reduction in the height of the flow passage. The value is insensitive to the shape assumed for the velocity profile. Surface roughness values were taken from standard tables for concrete pipes, 0.002 applying to medium rough concrete and 0.003 to rough concrete; the values for the GMS intake are not known, but may be somewhat less. The dramatic narrowing of the boundary layer due to the flow acceleration can be clearly seen in comparison to the constant pressure case, and in the visualization in Figure 7.

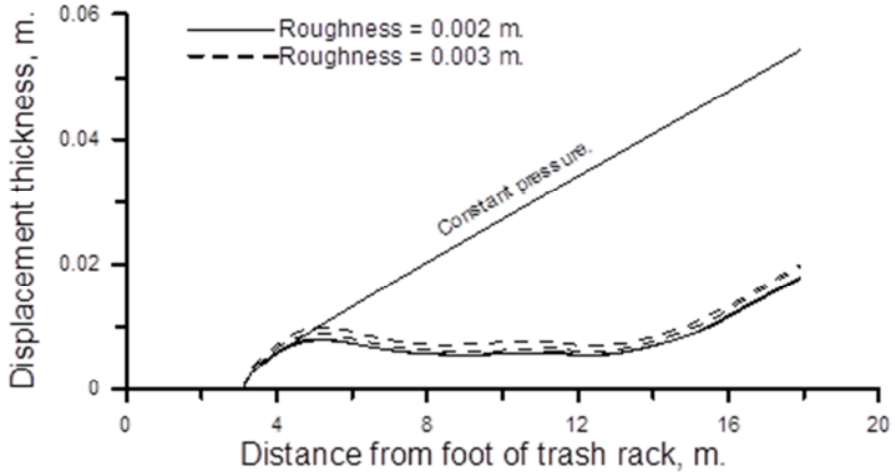

Figure 6. Displacement thickness distributions for the GMS intake.

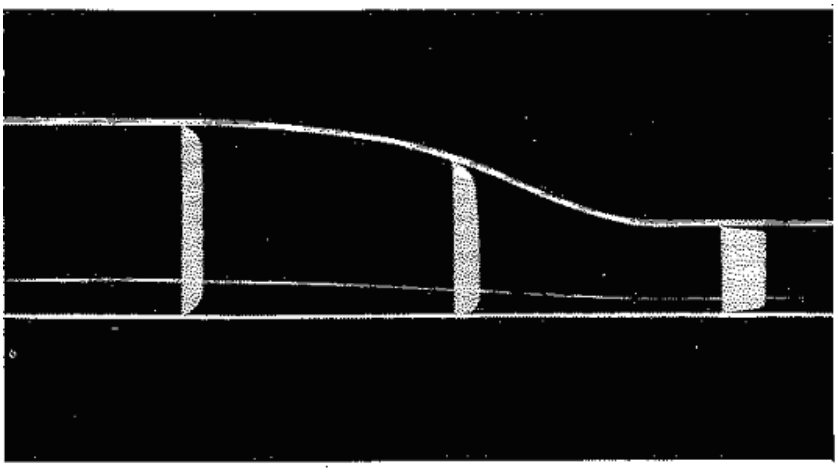

Figure 7. Image demonstrating boundary layer thinning in accelerating flow (Abernathy,1970).

The resulting displacement thickness at the measurement plane is shown in Table 1:

Table 1. Displacement thickness as a function of surface roughness

Roughness	0.002 m	0.003 m
δ^* (floor)	0.017 m	0.019 m
δ^* (roof)	0.018 m	0.020 m

The displacement thickness may be converted to a physical boundary layer thickness using a velocity distribution of the form $(z / T)^{1/n}$. The resulting integration recovers the displacement thickness. The displacement thickness and 1/n power law velocity profiles are related as follows,

$$T = \delta^* (1 + n) \qquad (5)$$

T being the equivalent physical thickness. The floor and roof boundaries initially used in the field (n = 4 and T = 0.30 m at the roof; n = 9 and T = 0.125 m at the floor) were replaced for both by n = 7 and T = 0.14 m.

Re-computing the discharges with these boundary corrections increased the AS flows by 1.2%: 0.4% from the adjustment to the roof elevation, with the remainder from the changes to the roof and floor boundary layers.

Flow Comparisons

Table 2 shows the discharges from each instrument for all of the measurement conditions, while Figure 8 shows the results for the three settings at which repeat runs were made.

Table 2: Comparison of discharges for AS and ATT instruments, all conditions

Test	Nominal MW	AS Flow cumecs	ATT Flow cumecs	% Difference (AS-ATT)/ATT*100
1	70	59.6	60.2	-1.0
2	93	73.5	74.0	-0.7
3	165	112.0	113.0	-0.9
4	186	122.0	123.2	-1.0
5	210	137.2	138.3	-0.8
6	230	149.2	150.4	-0.8
7	275	175.8	178.1	-1.3
8	185	122.0	123.0	-0.8
9	230	148.2	149.4	-0.8
10	190	124.4	125.4	-0.8
11	276	176.6	178.5	-1.1
12	276	176.6	178.5	-1.1
13	276	176.5	178.4	-1.1
14	230	148.8	149.7	-0.6
15	185	122.0	122.8	-0.7
16	185	122.4	122.8	-0.3
			Average Difference, %	**-0.9**
			Standard Deviation of Difference, %	**0.2**

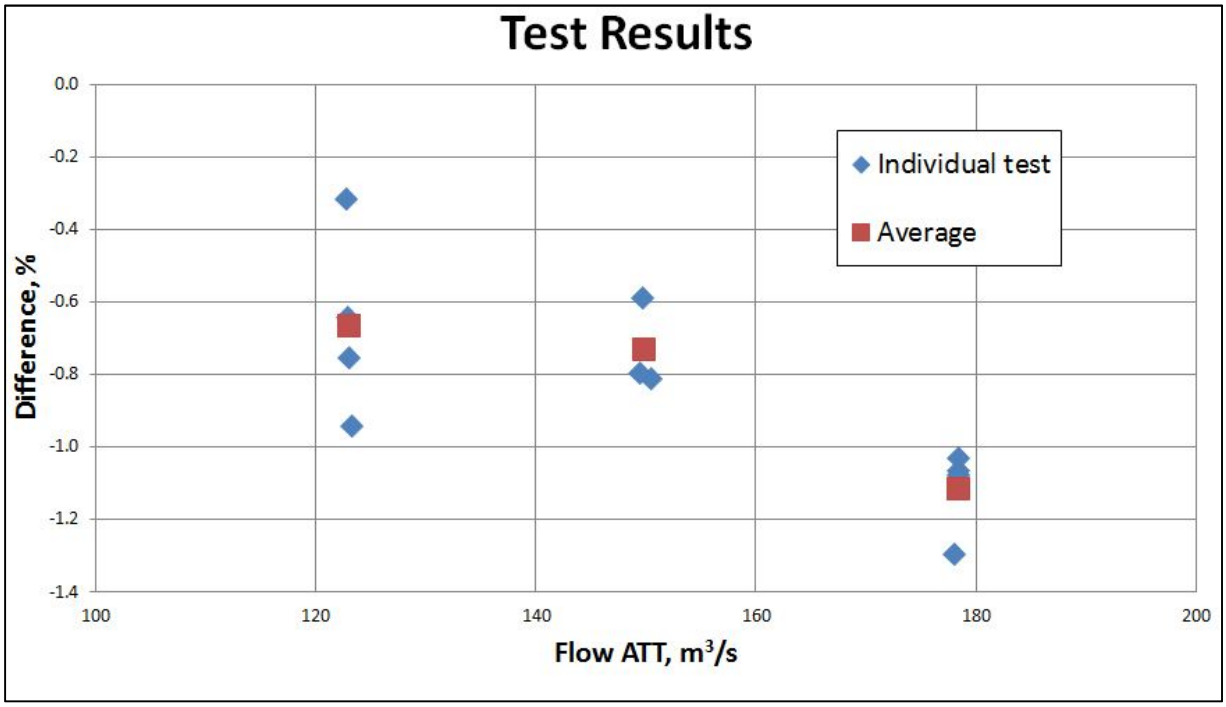

Figure 8: Average and individual differences between AS and ATT flows at each repeat setting.

The difference between the average discharges at each repeat setting is nearly constant at -0.7% for the two lower settings, but increases to -1.1% at the highest flow condition, however the scatter in the difference is greatest at the lowest flow.

These results are shown in more detail in Table 3, which shows the statistics of the flows measured by the two instruments and of the difference.

Table 3: Differences and Variability of the Two Methods

				% Difference		
Nom. MW	# runs	Q_{av} ATT (m^3/s)	Q_{av} AS (m^3/s)	Average	σ	Δ (95%)
185	4	122.95	122.13	-0.7	0.26	0.42
230	3	149.84	148.74	-0.7	0.12	0.31
276	4	178.36	176.36	-1.1	0.12	0.19

Nom. MW	σ_{ATT} (m^3/s)	Δ_{ATT} (m^3/s)	σ_{AS} (m^3/s)	Δ_{AS} (m^3/s)	σ_{ATT} (%)	Δ_{ATT} (%)	σ_{AS} (%)	Δ_{AS} (%)
185	0.18	0.28	0.19	0.30	0.14	0.23	0.15	0.24
230	0.52	1.30	0.51	1.26	0.35	0.87	0.34	0.85
276	0.19	0.30	0.40	0.64	0.11	0.17	0.23	0.36

The variability of the difference between the two methods is less than 0.5% at the 95% confidence level, and decreases with increasing flow, although the mean of the difference increases at the highest flow.

The variability of the flow measured by each instrument is similar at the two lower flows and slightly larger for AS at the highest flow. A plot of the deviation of the flow from the average at each repeat condition in Figure 9 shows that the majority of the variability for each method is from changes in the flow conditions, as they largely track each other from one repeat to the next (less so at the 185 MW setting).

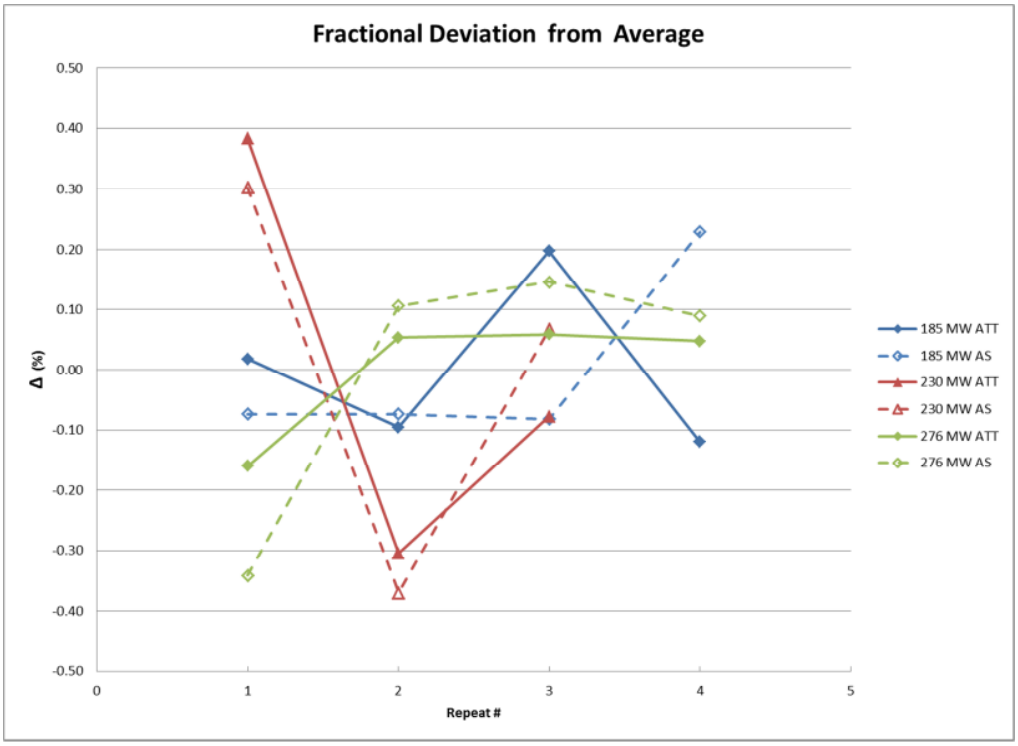

Figure 9: Fractional difference from the average flow for each repeat setting, AS and ATT.

Uncertainties of the Two Methods

The estimated uncertainty of the ATT method is ±1% when installed and operated in accordance with the requirements of the ASME PTC-18 Code (ASME, 2011). The difference between the AS and ATT flows ranged from -0.3% to -1.1%, with an average value of -0.9%.

The significance of the difference between the two methods may be evaluated through the normalized error, which is a means for assessing whether two measurements, both of which have associated errors, differ in a statistically significant sense (IEC, 2005). If, as is the case here, the error associated with one method is better known than the other, it also affords a way to estimate the less well-known error.

Here, we may define the normalized error, E_n, as

$$E_n = \Delta Q/(U^2_{AS} + U^2_{ATT})^{½} \quad (5)$$

If $|E_n| < 1$, then the two measurements are not significantly different. If we assume that U_{AS} is also ±1%, then E_n ranges from 0.2 for the minimum $|\Delta Q|$ of 0.3%, to 0.8 for the maximum $|\Delta Q|$ of 1.1%, and is 0.6 for the average $|\Delta Q|$ of 0.9%. The conclusion may therefore be drawn that the flow measured with AS in the intake are not significantly different than those measured by the ATT in the penstock, and have an uncertainty of no more than ±1%.

The geometry and velocity profiles for all 10 GMS turbine intakes will be the same, therefore the systematic component of the AS measurement uncertainty will also be the same. This means that the uncertainty in differences between units will depend largely on the random error, which for this test was indicated to be 0.5% of flow measured. Variations in measured flow are usually accompanied by changes in measured power. Therefore random errors in calculated efficiency (Power/Flow) would be much smaller than for flow, probably approaching ±0.2%.

Conclusions

The comparison test indicated that while the measurement uncertainty of the AS method is comparable to the uncertainty of the ATT method at ±1.0%, the anticipated uncertainty of the measurement at the 10 GMS units could be within as low as 0.2% if a sufficient number of repeats are undertaken. That is certainly sufficiently accurate for the dispatch optimization.

The test therefore confirms that BC Hydro is able to take advantage of the cost effectiveness of AS methodology for multi-unit testing at GMS.

Acknowledgements

The authors wish to thank the staff at the GM Shrum Station as well as the BC Hydro test personnel for their cooperation and assistance during the installation and operation of the ASFM. The boundary layer estimates were contributed by D. R. Topham, Topham Scientific Consulting, Victoria, BC.

References

Abernathy, Frederick H. 1970. *Film notes for Fundamentals of Boundary Layers*, National Committee for Fluid Mechanics Films, Harvard University, Cambridge, MA. (http://web.mit.edu/hml/ncfmf.html)

Almquist, C. W., J. W Taylor & J. T. Walsh 2011. *Kootenay Canal Flow Rate Measurement Comparison Test Using Intake Methods*. HydroVision 2011, July 19 – 22, 2011, Sacramento, CA

ASL Environmental Sciences Inc., 2001. *Acoustic Scintillation Flow Meter: Operating Manual for Advantage Model.* ASL Environmental Sciences Inc., Sidney, BC, Canada.

ASME 2011. *Performance Test Code PTC 18-2011, Hydraulic Turbines and Pump-Turbines.* American Society of Mechanical Engineers, New York, NY June 2011.

Clifford, S. F. and D. M. Farmer, 1983. *Ocean flow measurements using acoustic scintillation*. J. Acoust. Soc. Amer., 74 (6). 1826-1832.

Farmer, D. M. and S. F. Clifford, 1986. *Space-time acoustic scintillation analysis: a new technique for probing ocean flows.* IEEE J. Ocean Eng. OE-11 (1), 42-50.

IEC 2005. *General requirements for the competence of testing and calibration laboratories*. ISO/IEC 17025:2005. International Standards Organization, Geneva, 2005.

Schlichting, H., *Boundary Layer Theory*. McGraw Hill New York, 4th Edition, 1958.

Taylor, J., G. Proulx and J. Lampa 2012. *Turbine flow measurement in intakes – a cost-effective alternative to measurement in penstocks*. Hydropower & Dams, Issue 1, 2012, pp. 84 – 89.